Copyright is owned by the Author of the thesis. Permission is given for a copy to be downloaded by an individual for the purpose of research and private study only. The thesis may not be reproduced elsewhere without the permission of the Author.

Evaluating various classification strategies for identifying tree species for tree inventory creation from a hyperspectral image

A thesis presented in the partial fulfilment of the requirements for the degree of

Master of Science

In

Agriculture

at Massey University, Manawatū, New Zealand

Joel David Mackereth

2017

Summary

An inventory showing tree species locations is a valuable tool for urban forest managers to support a healthy ecosystem. Urban areas offer harsh environmental conditions for these trees. This intensifies the value of a tree inventory to make sure the urban forest provides environmental, social and economic benefits. But the frequency and coverage of an inventory can be limited due to cost, time, level of expertise and poor access to private property. This study aims to overcome this limitation by using hyperspectral remote sensing and analysis to create cost effective and relatively fast tree inventories that cover both private and public land. This research tests if this technology accumulates enough information to separate and classify twenty tree species within a diverse canopy.

To classify this image, this study used two stages. The first stage removed areas of the map that did not represent trees while the second stage separated twenty tree species from each other. This study used the aisaFENIX airborne imaging spectrometer to gather reflected light in the visible-shortwave infra-red (SWIR) range (400-2500 nm) over Palmerston North, New Zealand. The image has a 1 m^2 spatial resolution, 3.5-11 nm spectral resolution of 448 spectral bands. Then ground sampling of tree species locations collected correct training and accuracy testing data for the classifiers.

The classification compared 45 different strategies (9 pre-processing methods and five supervised classifiers). These combinations identified the best method to pre-process and classify the image at each stage. The pre-processing methods included band selection, and the noise reducing techniques of minimum noise fraction (MNF) and derivative reflectance (DR). While the classifiers used included the support vector

machine (SVM), binary encoding (BE), Mahalanobis distance (MHD), maximum likelihood (ML), and minimum distance (MD) classifiers.

The strategies produced vastly different results. In the first stage the MD classifier together with DR, MNF, and band selection pre-processing produced the best results when removing the non-tree surfaces from the image. In the second stage the SVM classifier together with MNF and band selection pre-processing achieved the best overall accuracy of 94.85% to separate twenty specific tree species. (Other tree species are misclassified as one of the twenty tree species). Therefore, this accuracy means that pixels representing each of the twenty tree species will be correctly classified within their own class 94.85% of the time.

Evaluating multiple strategies led to combination producing a high overall accuracy in being able to separate twenty tree species from each other. This shows that hyperspectral remote sensing could be an effective tool to create tree inventories in urban environments.

Acknowledgement

First, I would like to thank God who has guided me through this work. Second, I would like to thank my wife Ashlee Mackereth for being my number one supporter through it all. Also for providing while I completed this study and for encouraging me whenever I needed it. I would also like to thank my cousin Tommy Cushnahan for all the advice, help and time to talk about ideas and solutions. Also, thanks to Michael Dixon for the lunches over which we discussed our research and encouraged each other.

To Ian Yule, thank you for the opportunity to do this research and be a part of using innovative technology. Also, for giving me the freedom to make the research my own. To Reddy Pullanagari, thanks for the help with analysing the data and with accuracy testing.

To Marion MacKay, thank you for all the help with your tree expertise and keeping the research in the right perspective. Also, want to thank you for the many hours of discussion on the research as it helped me critique my own work.

Thanks to the various scholarship funding bodies: William Reed Scholarship (2016), Taranaki Tree Crops (2016 & 2017) and the Gosling Ornamental Horticulture Bursary (2016 & 2017) for the funding to help me through this research.

Table of Contents

Table of Figures

Table of Tables

1.0 Introduction

This research focuses on creating a cost effective and relatively fast method to obtain tree inventories in urban environments. This reduces the need to physically inspect and assess each individual tree which is time-consuming, costly, requires expertise and access to private property and entry in a Geographic Information System format. Hyperspectral remote sensing offers an alternative method to improve the process. The aisaFENIX airborne imaging spectrometer is a sensor that could give enough information for creating tree inventories. This method can reduce time requirements, increase overall effectiveness and give a comprehensive inventory of both private and publicly owned trees. If successful, someone can use this approach to analyse large areas to improve monitoring and management in urban forests. The location studied is Palmerston North, New Zealand with the Massey University Campus and Manawatu Golf Course being key survey sites.

This study focuses around four research questions:

1. Can a small training data set be used by different classifiers and how do they perform?
2. Is the shortwave infra-red (SWIR) range needed for correct classification?
3. Do pre-processing methods improve classifier performance?
4. Are the spectral signatures of different species found in a complex canopy sufficiently distinct to separate the species?

The hypothesis is that 'pre-processing and classification of information gathered by the aisaFENIX sensor will separate twenty tree species with an overall accuracy of >90% in an urban environment using a small training data set'.

2.0 Literature review

This review covers:

- The importance of the urban forest, and how it provides environmental, economic and social benefits.
- The difficulty managing biological diversity and tree populations in urban environments.
- The importance of tree inventories as key management tools for maintaining the urban forest. The traditional method and its drawbacks.
- The potential value of Hyperspectral remote sensing as an alternative method to improve upon the current method.
- Classifier and pre-processing methods for analysis of hyperspectral data.

In 2014, 54% of the world's population was living in urban environments and is expected to increase to 66% by 2050 (United-Nations, 2014). This trend of urbanisation throughout the world has led to large regions of urban developed landscapes (Samson, 2017). These landscapes have large proportions of sealed surfaces leading to less open and ventilated spaces, vehicular traffic, space heating and cooling and industrial processes (Samson, 2017). This results in high pollution levels in soil, water, air and vegetation removal (Samson, 2017). The urban forest is the remaining or planted vegetation that exists along urban streets, in parks, woodlots, abandoned sites, and residential locations (Alvey, 2006). These urban forests offer significant social, environmental and economic benefits (Bolund & Hunhammar, 1999; Jim & Chen, 2008; Morgenroth et al., 2016).

2.1 Benefits of the urban forest

Urban trees are the dominant natural feature in cities and they provide biodiversity and key ecosystem services which result in social, environmental, and economic benefits (Ordóñez-Barona, 2015). The health and diversity of the urban forest is a key influence on the benefits gained (Mullaney, Lucke, & Trueman, 2015).

Biodiversity and ecosystem services

Biodiversity in this study refers to the variability within and between tree species. Ecosystems services are the benefits that humans get from ecosystems which fall into four categories: provisioning, regulating, cultural and supporting services (Mace, Norris, & Fitter, 2012). Biodiversity is the underlying generator of these benefits and so ecosystem assessments include biodiversity because of its key role in ecosystem services (Mace et al., 2012).

Urbanisation causes a loss of biodiversity and therefore ecosystem services. This causes the remaining urban forest to become increasingly important to preserve both biodiversity and the services they generate (Alonzo, Bookhagen, & Roberts, 2014). Diverse urban forests mitigate this loss by positively influencing the diversity of fauna and the habitat, food and landscape connectivity (Rhodes et al., 2011).

Environmental mitigation

The urban forest removes gaseous pollutants such as nitrogen oxide, sulphur dioxide, carbon monoxide, carbon dioxide and ozone (Salmond et al., 2016). It also provides shading and insulation which reduces noise pollution (Baldauf, 2017) and fuel consumption for heating and cooling (Mullaney et al., 2015). Tree planting pits also

reduce storm water runoff by around 42% when compared with asphalt surfaces (Armson, Stringer, & Ennos, 2013).

Social

Urban forests and green spaces help reduce stress, anxiety and mental disorders through an emotional restorative response (Akpinar, 2016; Arnberger & Eder, 2015). They promote physical fitness (Coombes, Jones, & Hillsdon, 2010), improve the effectiveness of physical activity (Mitchell, 2013), decrease obesity (Wolch et al., 2011) and recovery time of surgical patients (Akpinar, 2016). These settings increase and encourage social interaction by providing an aesthetically pleasing location for citizens to view and be in (van Dillen et al., 2012). A study has also found the levels of crime decreased by as much as 50% in locations with high vegetation rather than low vegetation (Kuo & Sullivan, 2001).

Economic

Quantifying the economic benefits of the urban forest is difficult as they have no market value and are seen as liabilities instead of assets (McPherson, 2007). But, studies found that street trees reduce energy costs and increase business income and property values (Donovan & Butry, 2009; Pandit & Laband, 2010). The value of the removal of air pollution and reduction of storm water flow increases as the tree canopy cover increases (Mullaney et al., 2015). Taking these factors into consideration, studies estimated the annual net benefit per tree between US$21 and US$171 with an average of around US$50 (Mullaney et al., 2015).

2.2 Urban forest management

Preserving the health of trees in urban environments is difficult as the site conditions are less favourable compared with rural and natural regions. These have a negative influence on trees and can cause high mortality rates (Vogt et al., 2017) and a 30-40% lower life expectancy compared with rural landscapes (Schmitt-Harsh, Mincey, Patterson, Fischer, & Evans, 2013). As managers, it is important to know what influences exist in the region and how to manage them correctly.

Poor soil conditions such as compaction, hypoxia, water availability, unsuitable soil type, inadequate root space, nutrient deficiency, salinity and heavy metal concentration negatively influence tree health (Koeser, Gilman, Paz, & Harchick, 2014; Franco, Bañón, Vicente, Miralles, & Martínez-Sánchez, 2011; Nowak et al., 2004). This is also the case with root disturbance and restriction caused by construction works and utility trenching (Vogt, Watkins, Mincey, Patterson, & Fischer, 2015).

Poor above soil conditions such as high concentrations of air pollutants like carbon dioxide, ozone, and nitrogen oxide can damage leaf tissue (Vogt et al., 2017). Also tall buildings and structures can block direct sunlight reducing the light availability which slows the daily growth and weakens the plant's resistance of some species (Vogt et al., 2017). High temperatures speed up biological processes and the evapotranspiration rate which increases the demand of water leading to less moisture in the soil and increasing the vulnerability to water stress (Arnfield, 2003).

To increase the biodiversity of an urban forest to generate ecosystem services, stability and sustainability is important. However, because of the many negative influences that an urban environment has, certain species of trees are unsuitable and will not survive

(Mullaney et al., 2015). Managers should still aim to have <10% of the tree population as one species, <20% of a single genus and <30% of a single family (Morgenroth et al., 2016). This minimises the urban forests vulnerability to a parasitic invasion e.g. the emerald ash borer and Dutch elm disease (Arnberger et al., 2017, Clark & Matheny, 1991).

To manage these influences, a structured approach is ideal (Miller, 1997) which usually involves four key steps (Gibbons & Ryan, 2015). The first step is answering, 'What do you have?', where it requires a sound knowledge of the current state of the urban forest. This involves having a tree inventory to make decisions from and will be discussed in the following section.

2.3 Use of tree inventory to manage the population.

A tree inventory is the first step to effective urban forest management. Inventories offer essential information on forest cover (Ghosh et al. 2014), forest ecology and response to change (Lucas, Bunting, Paterson, & Chisholm, 2008), and aggregated data on individual trees such as species, location, health, size and age (Ghosh, Fassnacht, Joshi, & Koch, 2014). Managers use this data of what is present and absent in the urban forest to decide on diversifying, improving and preserving the tree population. Tree inventories also enable managers to form management goals and objectives, increase public knowledge and to secure funding and support (Alvey, 2006).

To get a tree inventory, traditional field surveying techniques of going to each tree and assessing it generates a limited tree inventory for many reasons. Firstly, it is labour-intensive e.g. it can take a trained, 2-person crew around 14 weeks to survey 200 0.04-ha plots (8 ha) (Nowak, Walton, Stevens, Crane, & Hoehn, 2008). Secondly, traditional

surveys are expensive but vary depending on the local transport and labour costs of the region (Alonzo, McFadden, Nowak, & Roberts, 2016). Thirdly, surveyors need permission to access privately owned trees (Alonzo et al., 2016). Fourth, if only a portion is surveyed and used to represent the whole urban forest then the important answer of 'what trees are where?' is limited to the survey locations. This is a problem as projections or estimations of what trees exist in the non-surveyed areas are not spatial explicit and are prone to sampling error (Alonzo et al., 2016). Spatially detailed data is ideal and important as knowing the location of each species allows managers to plan and monitor the diversity, composition and renewal of the population. It also facilitates management of threats such as pests, fire, and blight (Laćan & McBride, 2008; White & Zipperer, 2010). Therefore, alternative methods that achieve a comprehensive tree inventory with spatially explicit data, while also reducing labour, time and cost, would be ideal. Using remote sensing is a potential alternative method that will be discussed further in the following section.

2.4 Hyperspectral remote sensing

Remote sensing is where a non-contact sensor is used to measure the light intensity reflected by objects across the electromagnetic spectrum (Toth & Jóźków, 2016). This technology has had three main progressions, first panchromatic sensors which filter the visible range into one band. Second, multispectral sensors (Figure 1) that have a few discrete bands which filter ≥30 nm ranges which range across the visible, shortwave infra-red (SWIR), and longwave infra-red (LWIR). Third, hyperspectral sensors that have hundreds of continuous narrow (<10 nm) bands across the visible, SWIR, and LWIR. (Toth & Jóźków, 2016). Hyperspectral remote sensing has a greater separation of information compared with panchromatic and multispectral sensors so it has a high

potential to distinguish between different objects (Hardin & Hardin, 2013; Zhang & Mishra, 2012).

These bands are layered on top of each other forming a data cube which allows the reflectance values from each band to be assessed either individually or with the other bands. Hyperspectral sensors such as the aisaFENIX can have 448 layers and it is the

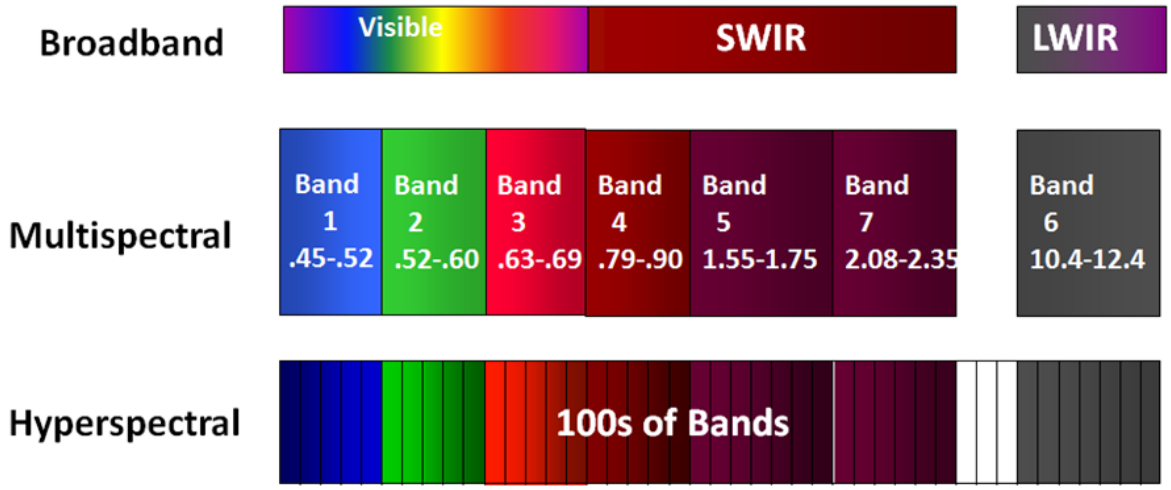

Figure 1: Difference between multispectral and hyperspectral data (Elowitz, 2016)

differences in the intensity of reflected light captured by the sensor for each layer that allows for distinguishing one object from another. This is more clearly seen in Figure 2 where it shows that difference in reflectance of five objects across the 448 bands of an aisaFENIX image. Classification methods can analyse these differences to associate pixels that have similar reflectance values together.

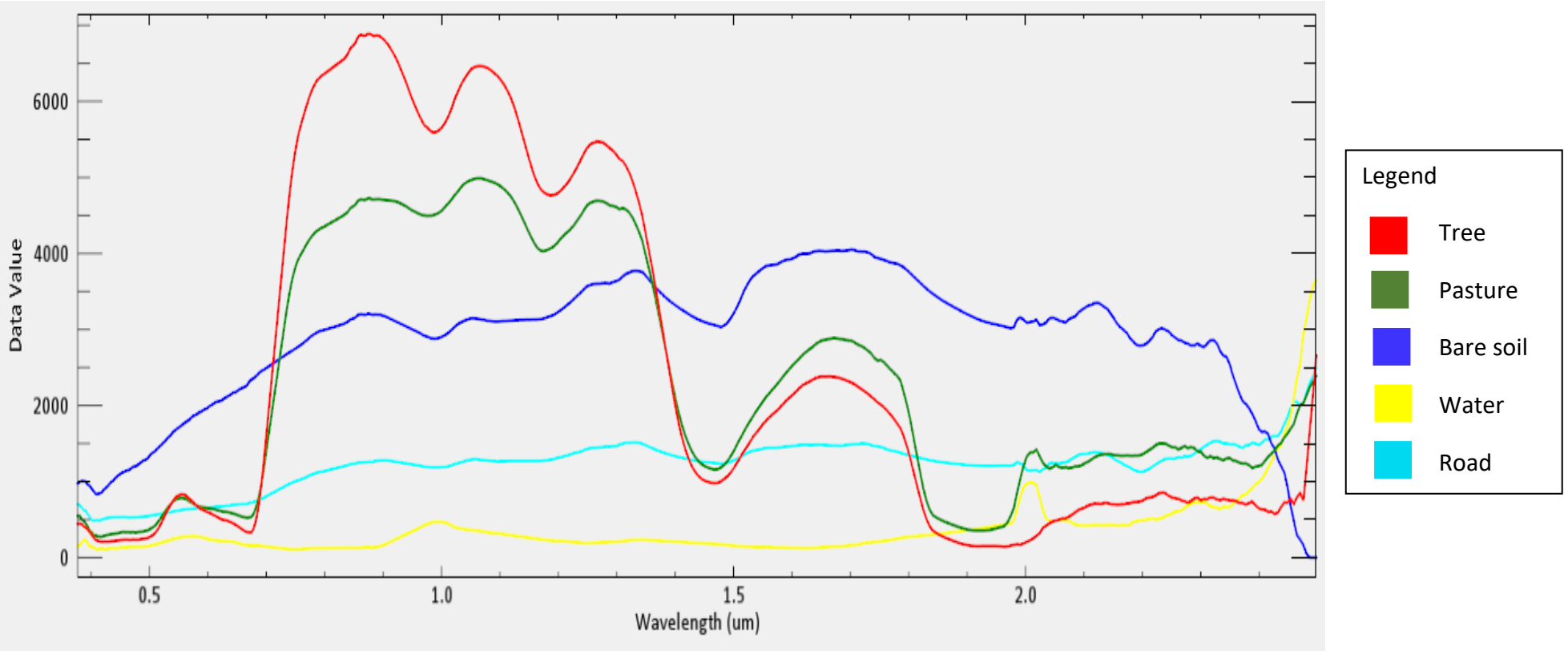

Figure 2: The measured light intensity of the five objects as observed by the aisaFENIX sensor

A sensor can be mounted on a satellite, an aircraft or on the ground (Fraser, Woods, & Brizzi, 2005; Martínez, Ortiz, Gil, & Rego, 2013). The spatial resolution from these platforms vary significantly depending on the instantaneous field of view and the distance from the object. Hyperspectral sensors on satellites, for instance, usually achieve 30 m^2 spatial resolution so spatial discernment of features within the image was difficult unless the object is larger than 30 m^2 (Toth & Jóźków, 2016). However, airborne hyperspectral sensors can provide fine scale spatial resolution information (≤ 10 nm) which significantly improves the clear discrimination of different small ground features (Lucas et al., 2008). For instance, HyMap (≈128 Bands) and AisaFENIX (≈448 Bands) are two airborne hyperspectral sensors, with the former achieving a spatial resolution of 1 m^2. The key factor is that the sensor resolution should be less than the size of the tree crown, which ensures that pixels do not include light reflectance from objects surrounding the tree crown. With the aisaFENIX sensor achieving a 1 m^2 spatial resolution and 448 bands when mounted on an aircraft it is suitable for tree species classification.

Hyperspectral remote sensing for tree inventorying

Using hyperspectral remote sensing instead of traditional surveys has many benefits. First, the sensor can measure difficult-to-access sites such as steep slopes and private property (Alonzo et al., 2016). Second, it will allow for examination of the connections between tree canopy and other spatial urban variables such as population, economic activity, or health. Third, regular repetitions of the same region allow managers to monitor the urban forest and detect changes. Last, this method only needs a few people to gather the data.

Previous studies have found that analysis of hyperspectral data can show a range of characteristics. It has been used to examine the relationship between health and reflectance (Treitz & Howarth, 1999), assess forest condition (Kefauver, Penuelas, & Ustin, 2012), biodiversity (Ghiyamat & Shafri, 2010), biomass (Koch, 2010), canopy nitrogen (Smith et al., 2002), age composition and classification of forests (Dalponte, Bruzzone, & Gianelle, 2008) such as Australian native tree species (Shang & Chisholm, 2014).

Using this technology to find tree species, has focused on North America and Europe regions with temperate forest ecosystems (Fassnacht et al., 2016). These studies vary in their approach and scale of research. The number of species examined usually ranged between 3-15 (Dalponte, Bruzzone, & Gianelle, 2012; Liu, Coops, Aven, & Pang, 2017) species with two studies using 29 species (Alonzo et al., 2016) and 40 species (Zhang & Qiu). Many involved using both hyperspectral and Lidar to identify the species. The hyperspectral results have overall accuracies ranging from 51 to 84.9% (Alonzo et al., 2016; Cho et al., 2012; Dalponte et al., 2012; Ferreira, Zortea, Zanotta, Shimabukuro, & de Souza Filho, 2016; Jones, Coops, & Sharma, 2010; Liu et al., 2017; Youngentob et al., 2011; Zhang & Qiu). A recent study using the aisaFENIX sensor in Israel identified 23 tree species to an overall accuracy of 82% and 86% for the two study sites. This study closely relates to the research proposed and supports the use of the aisaFENIX as an alternative method for tree species identification. This shows that discerning multiple species in a complex canopy is difficult to do but vital to this method being a practical alternative to just ground surveying.

The discussion of a general accuracy threshold has occurred in the past with Thomlinson (1999) suggesting that land-cover maps should have minimum accuracy requirements of 85% for overall accuracy with no class-specific accuracy below 70%. However, Foody (2004) iterates that instead of using a general accuracy needed for mapping, an accuracy minimum would vary based on the aim of the study. So, the better approach to decide at what accuracy a classification is successful should be determined at the beginning of the research.

The studies mainly use common validation methods to create training and validation samples, such as simple data splitting, x-fold cross-validation and bootstrap-sampling (Fassnacht et al., 2016). These methods use large proportions of their collected datasets to gain enough information to accurately classifying the samples. But, for this hyperspectral remote sensing method to be of most value, a small training data set is ideal (e.g. <10 trees per species) to reduce the size of the ground survey required and save on time and costs.

While it has been found that remote sensing can separate some tree species, there are multiple variations of techniques used within these studies. Different classifiers and pro-processing methods had variable accuracy results. They have made limited comparison between such classifiers and pre-processing techniques. However, the following section discusses some different classifiers and pre-processing methods that are the focus of this study.

2.5 Classifiers and pre-processing methods

Using supervised classifiers to analyse the spectral information gathered by the sensors to classify the tree species has been the basis of research in this field (Fassnacht et al.,

2016). There are many types of classification methods that analyse the data different and have been used to produce classifications for tree species (Fassnacht et al., 2016). Table 1 shows an example of such classifiers. these classifiers will assign each pixel to their nearest class unless a threshold exists is made.

Table 1: Description of different supervised classifiers

Classifiers	Description
SVM	The support vector machine classification is one of the most powerful classification techniques (Chen, Wang, Jiang, Yang, & Li, 2016). It analyses high-dimensional and noisy data (de Boves Harrington, 2017) to give correct and robust hyperspectral image analysis (Archibald & Fann, 2007). It does this by minimising the classification errors and maximising the difference between each class (Chen & Su, 2016). The SVM classifier performs well with small training datasets (Fassnacht et al., 2016) and usually outperforms traditional classifiers such as a maximum likelihood classifier (ML), minimum distance classifier (MD) and spectral angle mapper (SAM) (Du, Tan, & Xing, 2012).
BE	The binary encoding classification is a standard technique in classifying hyperspectral images. It reduces the data into zeros and ones based on whether a band reflectance is above or below the spectrum mean (Jia & Richards, 1993). This method is useful as it can reduce large data cubes while keeping most information (Xie & Tong, 2012).

MHD	The Mahalanobis distance classification is a classifier that measures the distance between two data points and tests the distance by setting different important factors to the features of data points (Xiang, Nie, & Zhang, 2008). It then assigns each pixel to the nearest class (Richards, 1999). This classifier is an effective and efficient way of classifying data but is vulnerable to bias with small samples and sensitive to the number of input variables (Fassnacht et al., 2016).
ML	The maximum likelihood classifier assumes the statistics for each class in each band are of a normal distribution and calculates the likelihood that a pixel belongs to a specific class (Richards, 1999). Like the MHD classifier, it assigns each pixel to the nearest class (Richards, 1999). But unlike the MHD classifier, it does not assume all class covariances are equal. This classification has the advantage that it is a consistent approach and is not biased in the presence of a larger sample set size (Fassnacht et al., 2016). However, this classifier assumes a Gaussian distribution of training data, and like the MHD classifier it is biased for small sample sets and is sensitive to the number of input variables (Fassnacht et al., 2016).
MD	The minimum distance classification is a technique that uses the average vectors of each endmember and calculates the Euclidean distance from each unknown pixel to the average distance for each class (Richards, 1999).

Hyperspectral images can be noisy in the light intensity across the spectrum. To reduce this noise and improve the classifiers ability to analyse this data the image can be pre-processed. There are many methods to do this; such as the minimum noise fraction (MNF) or converting it into derivative reflectance.

The minimum noise fraction (MNF) is a pre-processing method which creates principal component analysis rotations (Green, 1988). This method works by analysing the image to find the biggest distinction and removing it to put it into the first rotation band. The next rotation will use the remaining data to find the next biggest distinction and so on (Boardman, 1994; Green, 1988). MNF components have led to the best accuracies for tree species classification in the studies (Ghosh et al., 2014; Zhang & Qiu, 2012), although the studies found that reducing the number of bands reduces the accuracies (Dalponte, Ørka, Gobakken, Gianelle, & Næsset, 2013).

Another pre-processing method is converting the reflectance into derivative reflectance. This minimises the effects of background soil, illumination, surface albedo and by resolving the overlapping spectral features of vegetation biochemistry (Demetriades-Shah, Steven, & Clark, 1990; Schlerf et al., 2010). In other tree species classification studies, the use of derivatives like this one has always led to at least similar results but in most cases better results (Fassnacht et al., 2016).

2.6 Summary

The current body of knowledge agrees that, with urban regions expanding, trees in these environments are valuable for biodiversity and generation of ecosystem services to offer social, environmental and economic benefits. But, the literature also states that

urban regions offer a poor growing environment for trees compared with rural and natural environments. This means that managing urban trees to preserve tree health and diversity can be a difficult task. A tree inventory is a valuable tool to assist urban forest managers. The growing research field of hyperspectral remote sensing has shown that tree species can be accurately classified remotely to an extent. This technology might overcome the problems of time, cost, and access associated with the traditional ground-based inventory. If this technology could create tree inventories for urban managers, it would provide a tool to help them assess the whole urban forest and adjust their management plans.

While some research deal with tree species classification, there are gaps in the knowledge. Fassnacht (2016) and co-researchers compiled a review on hyperspectral remote sensing in tree classification which highlights some knowledge gaps that now exist within this field of research. Currently, most studies have used North America and Europe locations, with a few in South Africa and Australia (Fassnacht et al., 2016). There is little research on New Zealand locations, so conducting research in New Zealand will bring new evidence to the field to either support or add to the current body of knowledge. No study achieved an accuracy above 90% with just the use of hyperspectral data with twenty or more species. Also, many of these studies had no hypothesis, research question or pre-defined accuracy requirements (Fassnacht et al., 2016). Also, limited use or comparison of multiple pre-processing methods and classifiers during the study to verify the best approach was highlighted. So, analysing how different classifiers handle the same transformed information would add to current knowledge. To that

end, the research questions mentioned in 1.0 were formed to advance the current body of research and to fill the knowledge gaps that exist. These questions were:

1. Can a small training data set be used by different classifiers and how do they perform?
2. Is the shortwave infra-red (SWIR) range needed for accurate classification?
3. Do pre-processing methods improve classifier performance?
4. Are the spectral signatures of different species found in a complex canopy sufficiently distinct to accurately separate the species?

Also, the hypothesis that 'pre-processing and classification of information gathered by the aisaFENIX sensor will separate twenty tree species with an overall accuracy of >90% in an urban environment using a small training data set,' will, if proven true, answer these questions.

3.0 Study site

The city of Palmerston North (Figure 3), located in the mid-lower half of the North Island of New Zealand. This city contains a diverse urban forest of over 150 tree species making it a highly complex canopy.

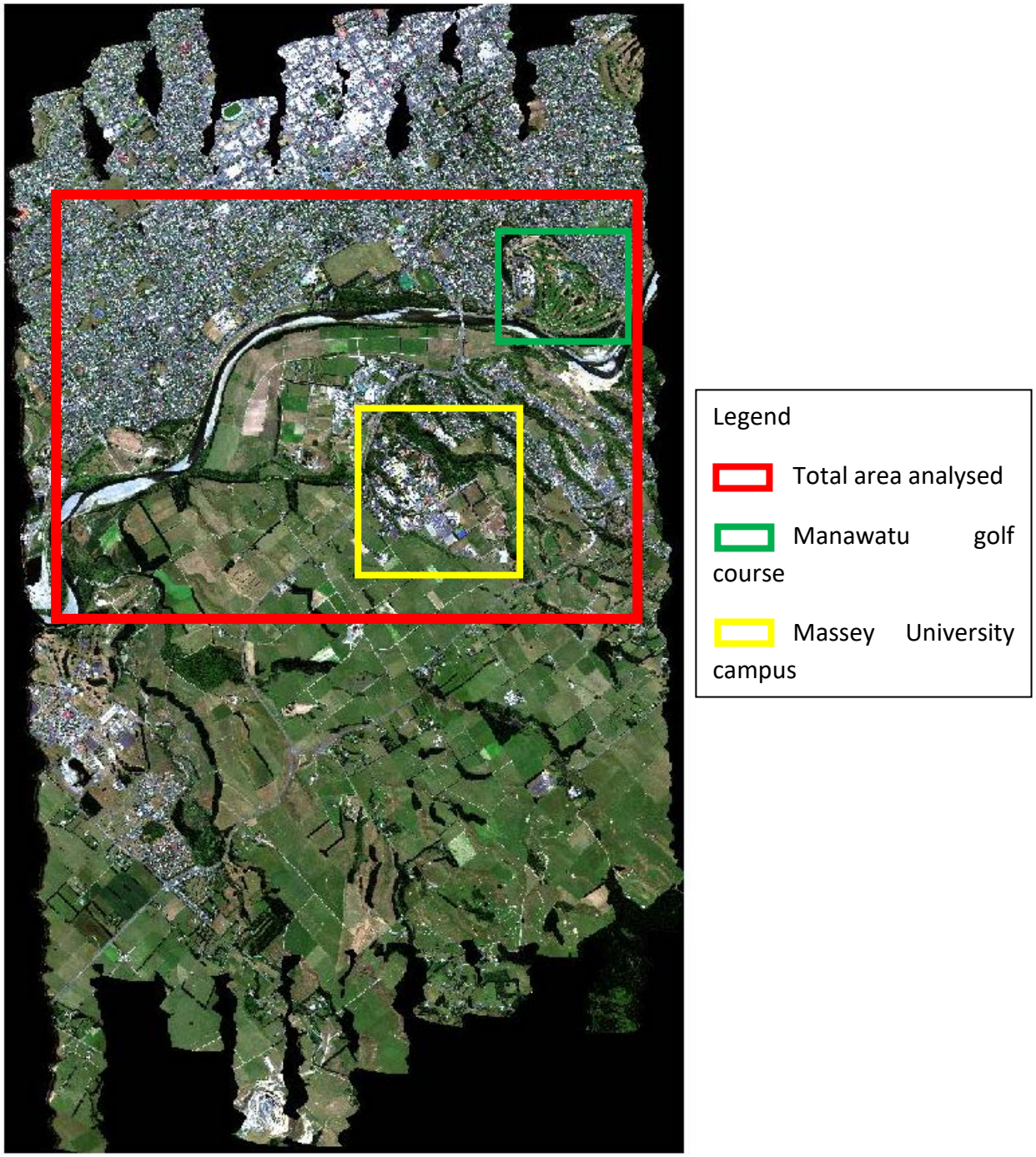

Figure 3: Aerial survey by the aisaFENIX

4.0 Stage one

The research was divided into two stages, the first focusing on removing the non-tree surfaces such as roads, grass and buildings from the image. This eliminated a large area from the image that was not the focus of the study, allowing further classifications to be more efficient. Also, this meant that in later classifications individual classes for these non-tree related surfaces were not required.

4.1 Methodology

Stage One had two phases. The first phase collected aerial survey data while the second phase analysed the data and produced classifications.

4.1.1 Aerial survey

This survey area covered the region of Palmerston North shown in Figure 4 which was gathered as described in Pullanagari, 2016. In brief, an AisaFENIX sensor (Specim Ltd., Finland) captured a single data cube of the 380 to 2500 nm spectral range at a 3.5-11 nm spectral resolution between 448 bands on the 22nd of February 2016 (Ogen, Goldshleger, & Ben-Dor, 2017). Applying radiometric correction, geo-rectification, atmospheric correction, mosaicking and spatial filtering on the data cube prepared the image for the second phase (Pullanagari et al., 2016).

4.1.2 Data analysis

The first stage of analysis goal is to remove non-organic (roads, water, roofs, cars, artificial turf, soil, shadow) and non-tree organic (Grass, crops and small plants) pixels from the data cube so that only trees remained. This research used five supervised classifiers (Harris, 2017): Support Vector Machine (SVM), Binary Encoding (BE), Mahalanobis Distance (MHD), Maximum Likelihood, Minimum Distance (MD) classifiers

because of their availability in the ENVI version 5.3 program (Exelis Visual Information Solutions, Boulder, Colorado) and their compatibility using the same training and accuracy testing data. Before using the classifiers, pre-processing methods (Alonzo et al., 2014) were applied to the image beforehand to improve the results by the classifier. The minimum noise fraction (MNF), derivative reflectance (DR) and band reduction are pre-processing methods used in eight different ways, as shown in Table 2.

Table 2: The pre-processing methods used to create the processed images

Name	Description
Unprocessed	The original data cube received after the first processing and spectral filtering described in section 4.1.1.
VIS	This image only has the bands that represent the visible spectrum (390-700 nm) which human eyes can see (Starr, Evers, & Starr, 2006). This sensor has 92 bands in this range.
MNF 100	This applies the MNF to 100 rotations to the Unprocessed image.
MNF 20	This applies MNF to 20 rotations to the Unprocessed image.
MNF 20 Inverse	This applies MNF to 20 rotations to the Unprocessed image and then inverted.
DR	This applies first derivative processing to the Unprocessed file.
DR MNF 100	This applies first derivative processing to the Unprocessed file. Then it applies MNF to 100 rotations to the DR image.
DR MNF 20	This applies first derivative processing to the Unprocessed file. Then it applies MNF to 20 rotations to the DR image.
DR MNF 20 Inverse	This applies first derivative processing to the Unprocessed file. Then it applies MNF to 20 rotations to the DR image and then inverted.

Training data and Accuracy testing data

Supervised classifiers need spectral information as training data from the image for each class to analyse and classify the image. In ENVI, the regions of interest (ROI) function was used to select equal numbers of pixels (Pham, Brabyn, & Ashraf, 2016) to create training data for each class (Figure 5). The pixels were manually selected with each class having 50 2x2 window ROIs which totalled up to 200 pixels for each class to be used for training the classifiers. A further 500 2x2 window ROIs (2000 pixels) for each class is used as accuracy testing data to independently validate the classifications accuracy of separating the three classes.

A small training dataset was used to reduce the ground sampling required for the classification and to increase the proportion used from the ground sampling for accuracy testing. This maximises the value for classes that have a few pixels associated to it e.g. if only 4/100 pixels are needed instead of 80/100 pixels it increases the accuracy testing size from 20 pixels to 96 pixels. Having a larger accuracy testing sample size improves how the accuracy results reflect the true accuracy. So, it was decided to use 200 pixels of each class to classify each image and 2000 for accuracy as the best-supervised classifier and image combination for this stage.

Accuracy interpretation

Accuracy represents whether the classifier correctly separated and assigned each of the 6000 pixels to one of the three classes correctly. This means that if an object (e.g. a tree) is in the image then it will be correctly classified into the Mixed Tree class based on that accuracy. However, if in the image there is an object that does not fit into any of the

three classes then it would be assigned to one of them, regardless. As over-classification occurs the technique only analyses how a classifier separated the pixels relating to each class. In cases of over-classification visual assessments or quantitative analysis cannot be conducted on the classified image. But, the three classes represent every object in the image.

Accuracy threshold

The aim of this classification is to create a mask in the next stage that removes most of the non-tree related pixels to make the next stage of classification faster. Following Foody (2004) discussions, this stage uses two different accuracy thresholds. A minimum accuracy threshold of >99% for the Mixed Trees class and >90% for the non-organic and non-tree organic classes. If multiple combinations achieve these two thresholds, then the combination that is the best at separating these classes will be chosen. The high overall accuracy of doing so for the Mixed Trees class ensures that one class contains nearly all tree related pixels while the other two classes have most of the non-tree related pixels.

Figure 4: Examples of 2x2 pixel regions of interest for the Non-Organic, Non-Tree Organic and Mixed Trees classes selected for training or accuracy testing.

4.2 Results

Table 3 shows the overall accuracies achieved by each classifier and pre-processed image combination. The ML x DR MNF 20 combination produced the highest overall accuracy of 99.27% followed by ML x MNF 20 (99.17%) and SVM x MNF 100 (90.00%).

Table 3: Stage one overall accuracy

Overall accuracy	SVM	BE	MHD	ML	MD
Unprocessed	98.25%	80.67%	*	*	86.27%
VIS	93.98%	59.80%	90.98%	95.43%	70.48%
MNF 100	99.00%	54.15%	97.38%	98.08%	98.08%
MNF 20	98.57%	67.67%	97.30%	99.17%	92.52%
MNF 20 Inverse	98.68%	84.03%	*	*	90.60%
DR	98.43%	79.60%	*	*	94.75%
DR MNF 100	98.65%	56.57%	97.43%	98.50%	92.52%
DR MNF 20	98.68%	55.98%	97.28%	99.27%	93.32%
DR MNF 20 Inverse	98.68%	89.65%	*	*	95.72%

* Unable to classify

The ML and MHD classifiers did not classify the Unprocessed, MNF 20 Inverse, DR and DR MNF 20 Inverse because they need more pixels than the image has bands. These images had 448 bands while each class had only 200 pixels. Out of the other images the ML classifier produced the highest classification across the classifiers for the VIS image with 88.6% while MHD produced the third highest with 90.98%. The rest of the transforms using MHD and ML all produced high accuracies ranging from 97-98% and 98-98.50% respectively. SVM produced consistent >98% results across all the images except for the VIS image (93.98%). The MD classifier results varied between 90-99% except for the VIS and unprocessed images which were below 90%. While the BE classifier achieved an accuracy between 55-90%.

The BE classifier performance improved with images that had more bands as shown by the four 448 band images producing accuracies between 79-89.65%. While the 100

band images ranged between 54-57%, the 92 band VIS achieved 59.80%, and the 20 band images between 55-68%. However, the SVM and MD classifiers usually produced better results with the lower band images.

In looking at the individual class accuracies for the three classes (Table 4), trends emerge in how the classes achieved higher or lower accuracies. With the Non-Tree Organic class, most of the combinations produced a higher accuracy than the other two classes. A few exceptions are combinations involving the ML classifier and the MD x DR and MD x DR MNF 20 Inverse whereby this class had the lowest accuracy. While this class accuracy performed poorly with the ML classifier, the opposite occurred with the MHD classifier combinations which produced the Non-Tree Organic class with the highest accuracy. The SVM and BE classifiers were more correct with this class while the MD classifier varied. The best accuracy of this class was 100% achieved by both the MHD x MNF 100 and MHD x DR MNF 100 combinations.

The Mixed Trees class was the next-best with the combinations including SVM, BE, MHD and MD producing either the second-best or worse class accuracy out of the three classes. However, it performed better with the ML Classifiers and produced the highest accuracy of the class of 99.55% with the ML x DR MNF 20 combination.

The Non-Organic class over the combinations produced the weakest accuracies. These largely came from the combinations that included the BE, MHD, and MD classifiers and many of the SVM combinations that included MNF processed images. It received better accuracies in comparison when the combinations included the ML classifiers. The highest accuracy (99.55%) was achieved from the SVM x MNF 20 Inverse.

Table 4: Stage one class accuracy

Combination	Non-Organic	Non-Tree Organic	Mixed Trees
SVM x Unprocessed	99.40%	98.65%	96.70%
SVM x VIS	99.25%	91.55%	91.15%
SVM x MNF 100	98.20%	99.80%	99.00%
SVM x MNF 20	96.95%	99.65%	99.10%
SVM x MNF 20 Inverse	99.55%	98.80%	97.70%
SVM x DR	98.60%	99.25%	97.45%
SVM x DR MNF 100	97.25%	99.90%	98.80%
SVM x DR MNF 20	97.35%	99.65%	99.05%
SVM x DR MNF 20 Inverse	98.35%	99.70%	98.00%
BE x Unprocessed	50.60%	97.75	93.65%
BE x VIS	25.75%	64.45%	89.20%
BE x MNF 100	52.90%	55.80%	53.75%
BE x MNF 20	76.70%	76.60%	49.70%
BE x MNF 20 Inverse	60.35%	98.50%	93.25%
BE x DR	69.80%	81.25%	87.75%
BE x DR MNF 100	59.25%	56.45%	54.00%
BE x DR MNF 20	58.85%	63.60%	45.50%
BE x DR MNF 20 Inverse	80.70%	95.85%	92.40%
MHD x Unprocessed	*	*	*
MHD x VIS	89.75%	96.50%	86.70%
MHD x MNF 100	93.90%	100.00%	98.25%
MHD x MNF 20	94.40%	99.80%	97.70%
MHD x MNF 20 Inverse	*	*	*
MHD x DR	*	*	*
MHD x DR MNF 100	94.25%	100.00%	98.05%
MHD x DR MNF 20	94.45%	99.80%	97.60%
MHD x DR MNF 20 Inverse	*	*	*
ML x Unprocessed	*	*	*
ML x VIS	98.60%	96.85%	90.85%
ML x MNF 100	99.15%	95.95%	99.15%
ML x MNF 20	99.35%	98.70%	99.45%
ML x MNF 20 Inverse	*	*	*
ML x DR	*	*	*
ML x DR MNF 100	99.40%	97.55%	98.55%
ML x DR MNF 20	99.45%	98.80%	99.55%
ML x DR MNF 20 Inverse	*	*	*
MD x Unprocessed	75.35%	90.25%	93.20%
MD x VIS	48.20%	74.60%	88.65%
MD x MNF 100	99.15%	95.95%	99.15%
MD x MNF 20	88.50%	99.60%	89.45%
MD x MNF 20 Inverse	81.05%	98.25%	97.00%
MD x DR	97.95%	88.85%	97.45%
MD x DR MNF 100	88.40%	99.70%	89.45%
MD x DR MNF 20	91.00%	99.60%	89.35%
MD x DR MNF 20 Inverse	98.80%	93.70%	94.65%

* Unable to classify

4.3 Discussion

In the method, two accuracy thresholds were set: >99% for Mixed Trees class and >90% for Non-Organic class and Non-Tree Organic class. With the Mixed Trees class being the most important, the combinations kept were ones that achieved the >99% threshold. Only six combinations achieved such a result and the others were removed from consideration (Table 5). While each of these combinations was above 99% the ML x DR MNF 20 produced the highest accuracy of 99.55%. These six combinations also achieved >90% accuracies for the other two classes. The ML x DR MNF 20 produced the highest Non-Organic class accuracy of 99.45% while the SVM x MNF 20 produced the highest Non-Tree Organic accuracy of 99.65%.

Table 5: The Mixed Trees class accuracy results with the combinations <99% removed.

Mixed Trees		BE	MHD	ML	MD
Unprocessed					
VIS					
MNF 100				99.15%	99.15%
MNF 20	99.10%			99.45%	
MNF 20 Inverse					
DR					
DR MNF 100					
DR MNF 20	99.05%			99.55%	
DR MNF 20 Inverse					

As all six combinations met the requirements to be used as a mask for an acceptable classification, the combination with the highest Mixed Trees class accuracy was used as a mask. Therefore, the ML x DR MNF 20 combination produced the highest mixed tree accuracy of 99.55% and therefore would be the mask for the second stage. This combination also produced the highest over the accuracy of 99.27% on top of high class accuracies (See Table 6).

Table 6: DR MNF 20 x ML accuracy summary

Class	Producers accuracy (%)	Producers accuracy (Pixels)
Mixed trees	99.55	1991/2000
Non-organic	99.45	1989/2000
Non-tree organic	98.80	1976/2000
Overall	99.27	5956/6000

The class statistics (see Table 7) show that the SVM has 0% of the image unclassified, as it classifies each pixel to the nearest class. As mentioned before, if there was an object in the image outside the scope of the three classes then the pixels representing this object would be assigned into one of these three classes. While this does not affect the classifiers ability to separate the three classes, it means that visual and quantitative interpretation of the classification could be misleading. However, for the Stage 1 classification this is not an issue. The total size of the image (Figure 4) sums to 17, 447, 535 m^2 pixels which represents 1,745 ha. The Non-Organic class is the largest region with 686 and 39.3% of the image. Mixed Trees is the next largest with 562 ha classified and 32.2% of the image. The Non-Tree Organic has 497 ha classified and 28.5% of the image. These high accuracy results give confidence that the classified regions size represents the true size. This supports past research in showing that a single flight can cover large regions of trees and classifying 562 ha of trees will provide valuable information for the urban forest manager to help quantify their management plans.

Table 7: DR MNF 20 x ML class statistics

Class	Pixel count	Percent (%)	Area (ha)
Unclassified	0	0	0
Mixed trees	5,617,700	32.2	562
Non-organic	6,859,525	39.3	686
Non-tree organic	4,970,310	28.5	497
Total	17,447,535	100%	1,745

These statistics also show it is possible to remove 67.8% (1,183 ha) of the image to just 562 ha of mixed trees to speed up future processing of the image. Comparing the classification to the colour image of the Massey University Campus (Figure 8) showed that the pasture and grass fields, surrounded by non-organic and mixed trees, matched the roads and tree lines surrounding them. The same was shown for the Manawatu Golf Course (Figure 8) where the classification showed the lines of trees separating the fairways and the sand bunkers located throughout the course. Another example of correct classification was the Manawatu River in the lower left corner where the river water and stones received the classification of Non-Organic.

Further analysis of the results showed that the VIS image in combination with the SVM classifier produced a good overall accuracy of 93.89% but was lower than the unprocessed image. This shows that the SWIR bands providing enough information to improve the result by 4.27%. This gap was larger in the BE and MD classifier comparison.

Using pre-processing improved the accuracy of every combination when classified by the SVM and MD classifiers. The improvement ranged between a 0.18-0.75% increase for SVM combinations and 4.33-11.81% increase for the MD combinations where in

both cases, the MNF 100 produced the highest improvement. BE classifier mostly produced lower results on pre-processed images than the unprocessed image. However, as noted in the results section, the images with 448 bands achieved higher accuracies than those with 100 or 20 bands. This suggests that the number of bands had more influence on the accuracy results than the pre-processing. Of the images that had the same number of bands as the unprocessed image, the MNF 20 Inverse and DR MNF 20 Inverse both improved the accuracy by 3.36% and 8.98% respectively. The derivative reflective processed image, however, had a 1.07% reduction in accuracy. Therefore, MNF pre-processing improved the BE classifier accuracy but even more so with both DR and MNF pre-processing. Combinations that failed to improve on the untransformed image should not be used in the future.

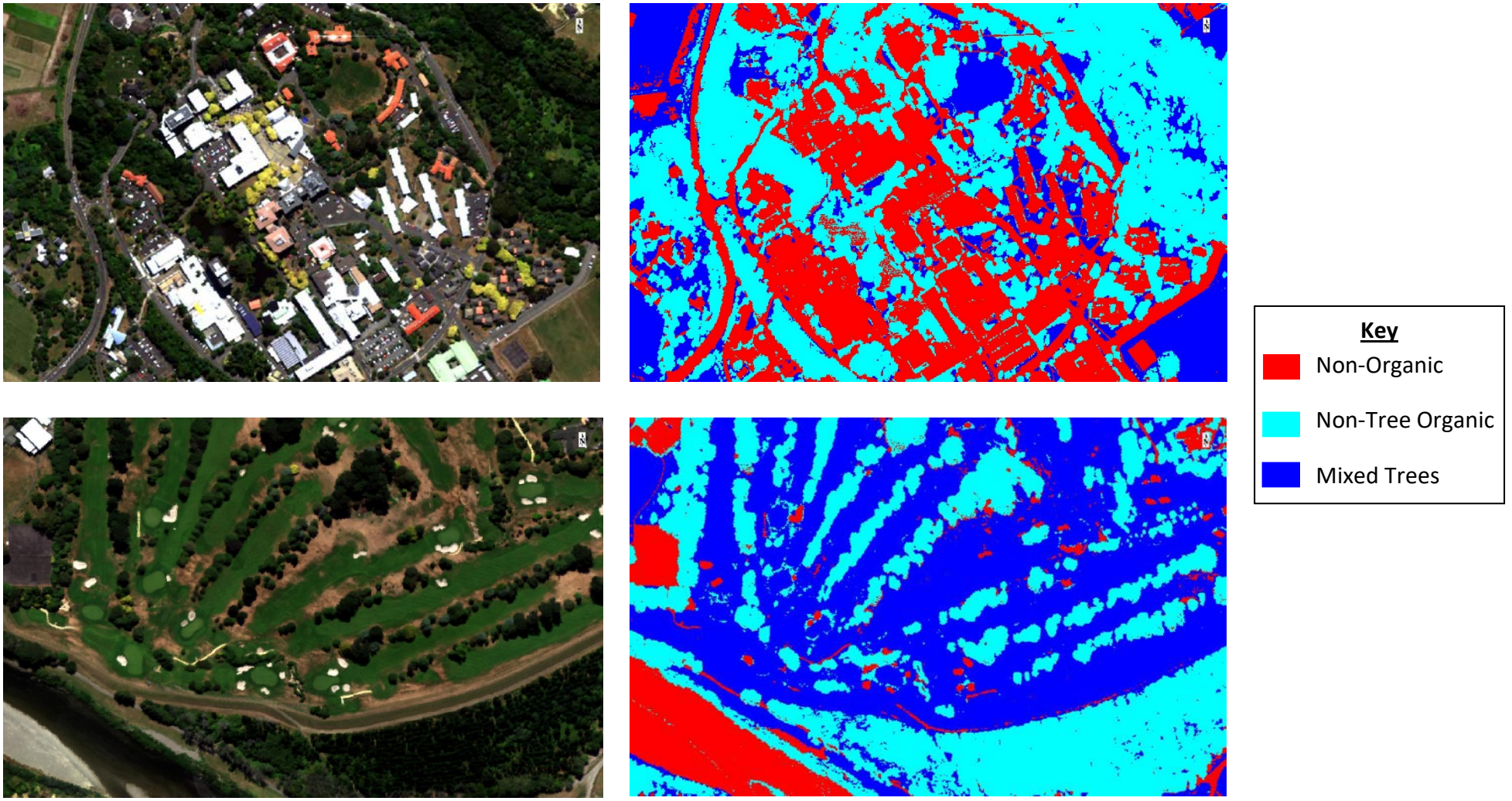

Figure 5: Stage one ML x DR MNF 20 classification image and colour image comparison, top right (Massey University Campus), top Left (Massey University Campus classification), bottom left (Manawatu Golf Course), bottom left (Manawatu Golf Course classification)

The classifiers SVM, BE, MHD, ML and MD were all quick to use and train using the regions of interest, unlike other classifiers such as Neural Net and SAM where other parameters are required to produce a correct result (Fassnacht et al., 2016). These classifiers varied in success, the MD and SVM classifiers produced good results, while the size of the training data constrained the MHD and ML classifiers.

Using small training sets was enough for many classifiers to accurately classify the image. The only main issue was that the training data size limited the MHD and ML classifiers. Most studies use the following statistical methods to select the ROIs mainly in a proportion of 70% for training and 30% for accuracy or 50/50 (Fassnacht et al., 2016). This stage only used 9.1% for classification and the rest for accuracy testing. If the region classified as these classes by the DR MNF 20 x ML classification were true, then the pixels used to train and classify the whole image (17, 447, 535 pixels) was 0.0034%. This supports the ability to use small regions of interest to train the classifiers to accurately classify the image. This shows that although Fassnacht, (2016) warns against small reference datasets as they may not represent the classification accuracy this not the case in this classification because of the larger accuracy dataset. It may become more of an issue with the tree species class reference datasets as there will be less area associated with each class.

A potential limitation to the accuracy testing method used in this work was that a stratified random sampling of the pixels selected from training data was not used. However, while the 200 pixels for each class in this stage were manually chosen for training the results should still be acceptable. A comparison between these two methods would be an interesting study for further work. Also, an alternative method to

test for accuracy would be to select the 2000 accuracy testing pixels by randomly selecting classified pixels from each classified image and ground truthing them. However, this was not considered because doing this for every 45 combinations would be labour extensive. It also limits the comparison between the combinations as they are not using the same sets of pixels.

Overall, the success of the ML x DR MNF 20 combination showed that analysing pre-processed images is a useful way to gain accurate classification of Non-Organic, Non-Tree Organic and Mixed Tree classes. While a small training dataset impeded some combinations from receiving a classification, for others, it was enough to achieve acceptable results, with most accurate being the ML x DR MNF 20 method.

5.0 Stage two

The second stage focused on using a series of classifiers and processing methods to analyse a complex canopy of mixed trees to identify and classify twenty tree species (Table 8).

Table 8: Tree species used as separate classes

Family	Latin name	Common name
Ulmaceae	*Ulmus glabra 'lutescens'*	Golden elm
Altingiaceae	*Liquidambar styraciflua*	Sweetgum
Fagaceae	*Fagus sylvatica*	Copper beech
Fagaceae	*Quercus palustris*	Pin oak
Fagaceae	*Quercus robur*	Common oak
Fagaceae	*Quercus rubra*	Red oak
Malvaceae	*Tilia x euchlora*	Lime tree
Myrtaceae	*Eucalyptus viminalis*	White gum
Myrtaceae	*Metrosideros excelsa*	Pohutukawa
Oleaceae	*Fraxinus excelsior*	European ash
Plantanaceae	*Platanus x acerifolia*	Plane tree
Salicaceae	*Salix alba var. vitellina*	Weeping willow
Sapindaceae	*Aesculus hippocastanum*	Horse chestnut
Ulmaceae	*Ulmus lobel*	Upright elm
Cupressaceae	*Cupressus x leylandii*	Leyland cypress
Cupressaceae	*Cupressus macrocarpa 'Goldcrest'*	Goldcrest macrocarpa
Cupressaceae	*Sequoia sempervirens*	Coast redwood
Pinaceae	*Cedrus atlantica 'Glauca'*	Atlas cedar
Pinaceae	*Cedrus deodara*	Deodar cedar
Arecaceae	*Phoenix canariensis*	Phoenix palm

5.1 Methodology

5.1.1 Ground survey

Unlike stage one, stage two needed a detailed ground survey to identify individual trees on the image, with this information being used in the classification of each tree species (Alonzo et al., 2014; Richter, Reu, Wirth, Doktor, & Vohland, 2016). In this study, the Palmerston North City Council provided access to their street tree database which provided identification and location of tree species on the city streets. Further ground surveys were conducted in early 2016 (midsummer) at the Massey University Campus and the Manawatu Golf course. Over 150 species were identified and their locations collated and used for data analysis.

5.1.2 Data analysis

This stage of classification used the same classifiers and processing methods as conducted in stage one. The non-tree surfaces were removed using a mask of the ML x DR MNF 20 classification. This classification has 20 different classes representing each of the tree species mentioned in Table 8. Six 2x2 window ROIs totalled up to 24 pixels were used to train the classifiers. The pixels were selected manually from the well-lit region of the tree crown of each tree species (Figure 11) to provide the strongest signal-to-noise ratio for classification (Fassnacht et al., 2016). A further 50 2x2 window ROIs (200 pixels) separate from the training pixels were selected over the image for independent accuracy testing of each class. This information trained and tested how well the combinations work to separate the twenty tree species from each other.

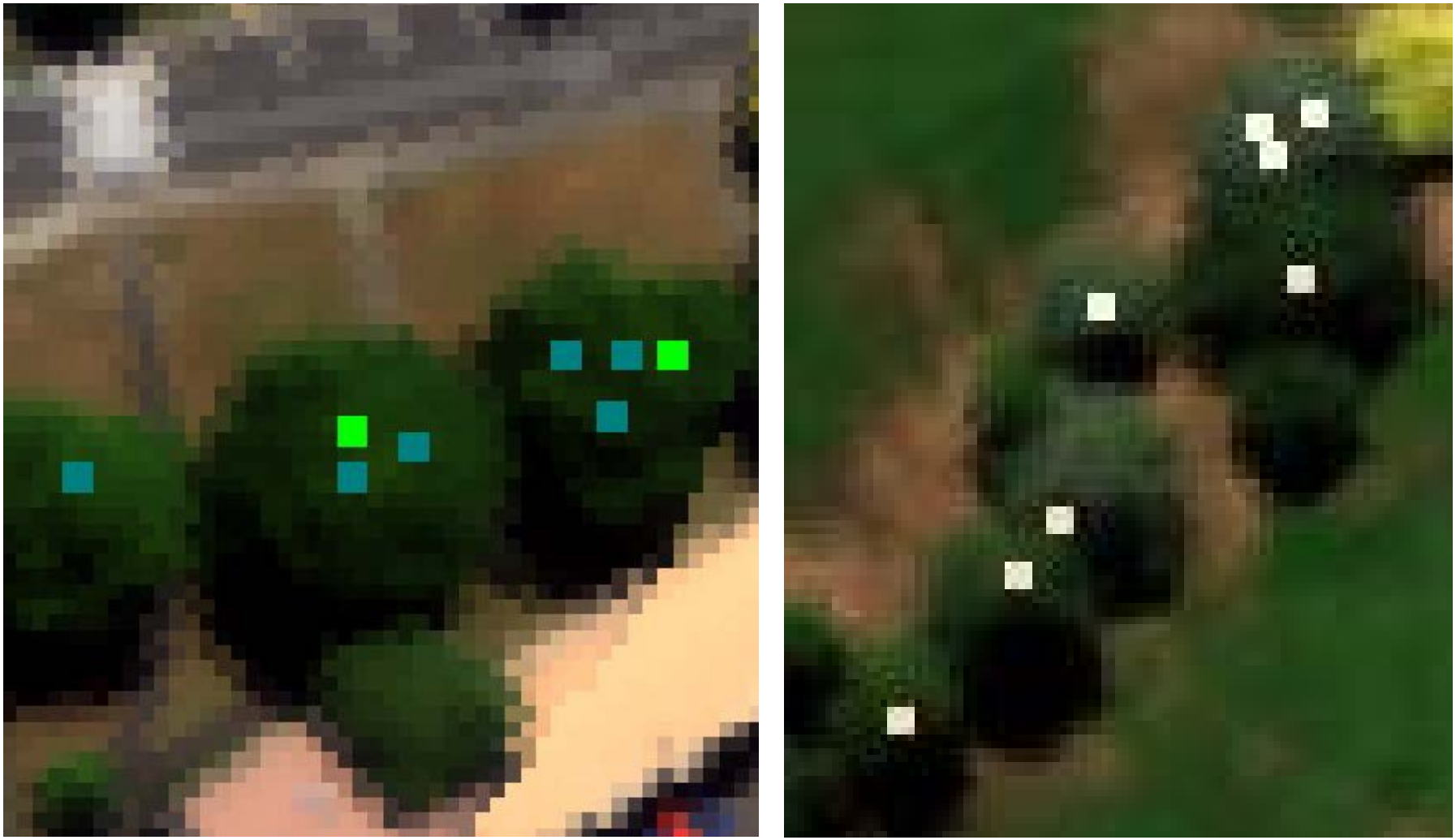

Figure 6: Regions of interest selected over the image for training and accuracy testing.

Accuracy interpretation

As mentioned in Stage One (4.1.2), over-classification can become an issue when all objects in the image do not fit into the classes being classified. While in Stage One it is not important, in Stage Two it has a larger impact on the usability of the results. Only twenty tree species classes were made while all the other tree species (150+) are then classified as one of the twenty classes. This means it limits the visual assessments or quantitative assessments of the classified image due to the area classified as one tree species could be a mix of multiple other tree species. Which is why, for this stage, classified images or quantitative analysis of the area classified was not shown as they can be misleading. Instead, the focus was on how well the classifiers split the twenty different targeted tree species apart. Therefore, accuracy in this stage will be defined as the ability of the classifiers to correctly put a pixel representing one of the twenty tree species into the class it represents. For example, a golden elm pixel is put into the Golden Elm class instead of the other 19 classes.

Accuracy threshold

The aim of this classification was to separate twenty individual species. As discussed in 4.1.2, there is a need for setting an accuracy threshold that will evaluate the success of failure of a classification. In past studies overall accuracy has ranged between 51-84.9% and few of these used twenty or more species. An overall accuracy threshold of 90% of the twenty species was set, as a high accuracy is required if using this method for to create a useful inventory. This threshold if met, would improve upon the current body of research for using hyperspectral remote sensing alone to classify tree species. The highest overall accuracy will determine the best combination.

5.2 Results

5.2.1 Overall accuracy

With accuracy defined in 5.1.2, the overall accuracy of stage two (Table 9) showed a greater variability in accuracy percentages and highlighted the limitations of some classifiers. Only the SVM and MD classifiers achieved classifications above the 90% overall accuracy threshold, with the SVM x MNF 20 combination producing the highest overall accuracy of 94.85%. It was also the only combination to achieve >90% class accuracies for 18 or more classes. The SVM classifier only produced two combinations with accuracies above 90%, the rest (excluding VIS) ranged between 68-89%. The MD classifier produced the highest number of accuracies >90% with four different combinations while other combinations accuracy dropped significantly.

Table 9: Stage two classification overall accuracy results

Overall accuracy	SVM	BE	MHD	ML	MD
Unprocessed	68.10%	21.30%	*	*	25.38%
VIS	45.03%	28.30%	*	*	34.78%
MNF 100	88.25%	62.03%	*	*	90.98%
MNF 20	94.85%	63.30%	83.65%	#	91.58%
MNF 20 Inverse	69.70%	36.68%	*	*	34.68%
DR	78.55%	24.68%	*	*	23.93%
DR MNF 100	82.13%	61.95%	*	*	91.23%
DR MNF 20	94.28%	61.25%	83.03%	#	91.08%
DR MNF 20 Inverse	88.68%	57.68%	*	*	45.88%

* Unable to classify
# Classification error

The BE classifier overall accuracy varied over the images with the highest being 63.30% with MNF 20. In this stage the images with fewer bands had higher accuracy which was the opposite result to that found in the first stage of classification. The SVM and MD classifiers experienced the same result as the MNF 20 and DR MNF 20 combinations and produced higher accuracies than those with high band numbers.

The MHD classifier only worked with two combinations, which had similar results of just above 83% with the MNF 20 image outperforming the DR MNF 20 image by 0.62%. The ML classifier could not classify any image because of the small training data size and classification processing errors.

5.2.2 Classifier accuracy

Instead of looking at the results for each individual combination, the results highest overall accuracy for each classifier and image will be highlighted (Table 10). All the classifiers (excluding ML) produced their highest accuracy when combined with the MNF 20 transform.

The best classifier (Table 10) is the SVM classifier followed by the MD, MHD, BE classifiers. The SVM x MNF 20 combination produced the highest overall accuracy of 94.85% and the 18 classes above 90% with 12 of them >95%. Only the Horse Chestnut (86%) and Upright Elm (83%) classes have accuracies below the threshold but were still moderately high.

Table 10: The best combination for each classifier (Accuracy definition see 5.1.2)

	SVM x MNF 20	BE x MNF 20	MHD x MNF 20	MD x MNF 20
Overall accuracy	94.85%	63.30%	83.65%	91.58%
Golden elm	100%	100%	94%	100%
Sweetgum	92%	39%	78%	87%
Copper beech	99%	100%	87%	99%
Pin oak	99%	54%	83%	99%
Common oak	96%	42%	80%	79%
Red oak	99%	51%	71%	80%
Lime tree	91%	70%	84%	93%
White gum	93%	66%	80%	91%
Pohutukawa	100%	93%	79%	97%
European ash	93%	56%	92%	92%
Plane tree	91%	91%	91%	93%
Weeping willow	100%	66%	96%	100%
Horse chestnut	86%	61%	76%	71%
Upright elm	83%	37%	70%	76%
Leyland cypress	100%	99%	99%	100%
Goldcrest macrocarpa	91%	43%	74%	96%
Coast redwood	96%	45%	79%	94%
Atlas cedar	98%	65%	88%	98%
Deodar cedar	96%	56%	77%	93%
Phoenix palm	100%	37%	100%	98%

Class accuracies >90% are highlighted in green

The MD x MNF 20 produced an overall accuracy of 91.58% with 15 of the classes above the 90% threshold with the remaining classes of Sweetgum, Common Oak, Red Oak, Horse Chestnut, and Upright Elm between 71-87%. The MHD x MF 20 combination produced an overall accuracy of 83.65%. This combination only produced six class accuracies above 90%, while the remaining 14 classes ranged between 70-88%. The BE classifier has the lowest overall accuracy of 63.30% but still produced five classes above the 90% threshold while the rest of the classes ranged between 37-70%. There is a wide gap between the 91% accuracy of the plane tree and the next highest of the Lime Tree class at 70%.

The SVM coupled with the MNF 20 image produced the highest result and is the best classifier for tree species classification followed by the MD classifier. The other classifiers failed to produce high enough accuracies or were limited by the training data.

5.2.3 Image accuracy

The comparison between the Unprocessed and VIS images (Table 11) show they produced their highest accuracies with the SVM classier of 68% and 45% respectively. Only the Unprocessed combination achieved a class accuracy above 90% with the Leyland Cypress class of 93%. The SVM x VIS combination was superseded by the Unprocessed image which had bands in the shortwave infra-red (SWIR)

Pre-processing methods, as opposed to using the unprocessed data (Table 11), achieved their best results with the SVM and MD classifiers. The starting point to measure any improvement is the SVM x Unprocessed which has an overall accuracy of 68% and one class above 90%. The SVM x MNF 100 combination produced a 91% overall accuracy with 13 classes, which is considerable higher than the SVM x Unprocessed classification.

However, the SVM x MNF 20 did even better with an overall accuracy of 95% and 18 classes above 90%. This shows the MD classifier produced a better result than the SVM with the MNF 100 transform but the SVM produced a higher overall accuracy with the MNF 20 transform. The MNF 20 Inverse produced its highest accuracy with the classifier SVM but at a low overall accuracy of 70% which is barely better than the Untransformed combination.

The DR x SVM improved on the Untransformed combinations overall accuracy by 11% and had three classes above 90%. While the DR MNF 100 x MD combination reached an overall accuracy of 91% with 13 classes above 90% which reflects a similar result to that of the MNF 100 x MD combination. The DR MNF 20 x SVM combinations overall accuracy was 94% with 17 classes above the 90% threshold, which is slightly worse than its non-DR processed image counterpart. While the DR MNF 20 Inverse combination fell short of the accuracy required set in the methods with an overall accuracy of 89% with 11 classes above 90%.

Table 11: The best combination of each transformation (Accuracy definition see 5.1.2)

	Unprocessed x SVM	VIS x SVM	MNF 100 x MD	MNF 20 x SVM	MNF 20 Inverse x SVM	DR x SVM	DR MNF 100 x MD	DR MNF 20 x SVM	DR MNF 20 Inverse x SVM
Overall accuracy	68%	45%	91%	95%	70%	79%	91%	94%	89%
Golden elm	83%	86%	100%	100%	83%	89%	100%	100%	93%
Sweetgum	68%	20%	85%	92%	58%	66%	79%	86%	80%
Copper beech	86%	84%	100%	99%	82%	97%	100%	98%	96%
Pin oak	85%	13%	99%	99%	77%	82%	99%	100%	94%
Common oak	58%	19%	88%	96%	69%	59%	85%	94%	80%
Red oak	63%	57%	80%	99%	67%	66%	81%	99%	82%
Lime tree	78%	57%	93%	91%	75%	84%	92%	90%	86%
White gum	77%	76%	96%	93%	79%	87%	98%	93%	93%
Pohutukawa	63%	20%	99%	100%	58%	73%	99%	98%	85%
European ash	68%	72%	93%	93%	72%	83%	93%	93%	85%
Plane tree	89%	31%	93%	91%	86%	89%	93%	93%	91%
Weeping willow	55%	60%	100%	100%	81%	69%	100%	99%	92%
Horse chestnut	74%	15%	77%	86%	58%	82%	77%	84%	84%
Upright elm	40%	38%	67%	83%	49%	56%	68%	82%	84%
Leyland cypress	93%	27%	100%	100%	96%	91%	100%	100%	93%
Goldcrest macrocarpa	85%	78%	95%	91%	79%	91%	96%	91%	88%
Coast redwood	61%	47%	88%	96%	65%	81%	88%	95%	94%
Atlas cedar	56%	51%	86%	98%	52%	67%	89%	98%	90%
Deodar cedar	64%	40%	92%	96%	61%	80%	96%	98%	90%
Phoenix Palm	20%	15%	96%	100%	52%	84%	98%	100%	98%

Class accuracies >90% are highlighted in green

5.3 Discussion

Interpreting the results of Stage Two differs significantly from Stage 1. Although the non-tree surfaces were removed, over-classification was present in this classification as there are over 150 tree species within the area that was classified as Mixed Trees. This means that visual and quantitative assessments would mislead in that the class area has species other than the twenty-targeted species. An example of this is in Figure 10 where the classified area of the Copper Beech class also includes *Prunus cerasifera x blireiana* (Flowering plum) and *Acer platinoides* 'Crimson King' (Norway maple).

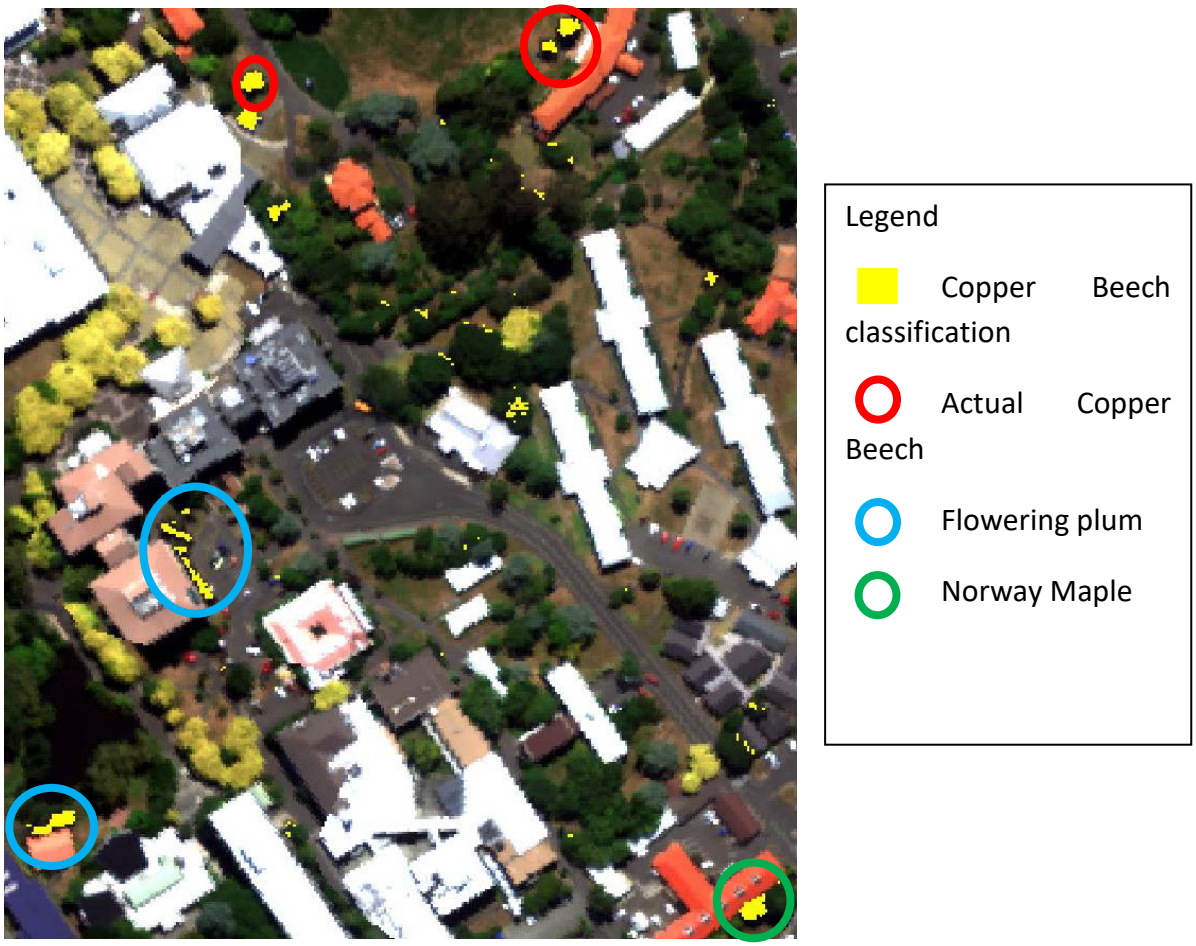

Figure 7: Over-classification of the Copper Beech class

To overcome this problem in the future, alternative methods could be used. Firstly, you could add a class for every single tree species in the image. While this is a simple method, it was not practical as many of the species had few examples from the ground survey. Secondly, you could create a single or few extra classes that grouped multiple species into them which would avoid them being over-classified in the other twenty classes. However, the ground survey of tree species may not include all the tree species causing some species to be still misclassified. Another issue with this method is that merging distinct species together can lead to unusually averaged spectra which could be similar enough for increase misclassification in other classes. While adding a class for each species is ideal, it can be difficult in a highly diverse canopy that has over 150 tree species. So, for the interpretation of this classification the focus was on being able to separate the twenty-tree species from each other and not about creating a classification that only included the twenty-tree species. However, future work could be done on adding more classes to make the classification more specific for practical visual and quantitative analysis.

With the high threshold set, the SVM x MNF 20 combination outperformed against the other combinations. It separated the tree species to an overall accuracy of 94.85% and class accuracies above 90% for 18/20 classes. However, the Horse Chestnut and Upright Elm classes only achieved 86% and 83% accuracies, respectively. There are a few reasons that could cause these species to receive lower accuracies. First, earlier research has considered

the spectral similarity between tree species is too high for the correct distinction between them (Alonzo et al., 2014; Ghosh et al., 2014; Lucas et al., 2008; Zhang & Mishra, 2012). However, it is unlikely as the Pin, Common and Red Oak classes have accuracies of 99%, 99%, and 96% respectively and they would share greater likeness than these two species. Second, pre-processing causes the loss of vital information leading to poor classification, but this would affect every class.

Figure 8: Accuracy ROI pixels chosen for horse chestnut (Top) and upright elm species (Bottom)

Third, bad training and accuracy regions of interest (ROI) caused the misclassification. Figure 12 shows the trees used for the regions of interest are trees with small width size. This means that many pixels used for the Horse Chestnut and Upright Elm classes were from small trees representing 4-5 pixels. The reason the canopy cover being small is important is that at a 1 m^2 resolution, the pixels around that edge of the trees could include partial reflectance from non-tree surfaces. This mix of surface reflectance creates noise leading to misclassification. The Horse Chestnut class had problems because

some trees were young and had a small canopy while the Upright Elms trees grow in a columnar shape causing the canopy to be small. The canopy size is accepted as the main reason for the lower classification accuracy. In future research, careful choice of training and accuracy testing ROIs will reduce misclassification.

Using pre-processing showed that it is an effective method to improve the accuracy of tree species classification. The MNF 20 pre-processing method has the most significant influence on improving the accuracy. The SVM x MNF 20 combination has a higher overall accuracy of 27% and 17 more class accuracies above 90% over the SVM x Unprocessed combination.

When images already had MNF applied, the DR had little impact on increasing the accuracy, with a minor decrease of accuracy in the DR MNF 20 x SVM combination. But the DR had an accuracy improvement of 11% when solely applied to the Untransformed image. The MNF 20 Inverse only slightly improved over the SVM x Unprocessed image when transformed first into DR it increased the overall accuracy by 19%. This shows when the image is pre-processed with DR it provides better information for discernment of tree species after undergoing 20 rotations of MNF and then inverted. Regardless, the best pre-processing method was the MNF 20 image.

The small training sets were enough for the classifiers to use to accurately identify 18/20 species to an accuracy of over 90%. This supports the ability to use small regions of interest per class to train the classifiers to accurately classify the image. Also, the BE classifier had

the worst results compared with the SVM and MD classifiers but achieved classifications of each image unlike the MHD and ML classifiers. The VIS image was inferior to the unprocessed image showing the depth of information the SWIR range provides for tree species classification. This is a key finding that supports using hyperspectral remote sensing is a practical alternative to traditional methods for tree inventorying. Only needing a few examples per class means that the ground work required is drastically reduced. However, while a small sample set was successful here, future research is needed to determine how many samples are needed per species and whether the sample size required varies between species.

6.0 Conclusion

This study set out to answer the four questions below.

1. Can a small training data set be used by different classifiers and how do they perform?
2. Is the shortwave infra-red (SWIR) range needed for accurate classification?
3. Do pre-processing methods improve classifier performance?
4. Are the spectral signatures of different species found in a complex canopy sufficiently distinct to accurately separate the species?

Training data

Minimising the size of the training data reduced the ground sampling area required without compromising the accuracy of the classification. Accuracies above 90% were obtained regardless of the small training sample. While the small size restricted the Mahalanobis distance and maximum likelihood classifiers, the support vector machine classifier and minimum distance classifiers could still achieve >90% overall accuracies. The binary encoding classifier could not achieve an accuracy as high due to either insufficient training information or inadequate classification method of the classifier. It is imperative that careful selection of training and accuracy pixels is done to prevent actual and false misclassification. Having a smaller training data reduces the ground survey requirements and increases the proportion of the pixels available for accuracy and therefore increasing the true accuracy of the classification.

Spectra range

Limiting the classifiers to using only the bands representing the visible range also limited the overall accuracy achieved. The SWIR range captured by the sensor provides essential information to improve the accuracy in both stages compared with just the visible range. While some good accuracies were obtained by the VIS image, it was outperformed by the Unprocessed image with all 448 bands. Therefore, to improve classification accuracies of non-organic, non-tree organic, mixed tree surfaces as well as individual tree species, the full range of the aisaFENIX should be used. This supports the importance of the shortwave infra-red range in providing distinct information for the improved classification of images.

Pre-processing methods

Pre-processing methods improve the classification of aisaFENIX images by removing noise and highlighting differences. The derivative reflectance improved the classifications but was outperformed by applying minimum noise fraction rotations. Using the pre-processing method MNF to 20 rotations was identified as the optimal pre-processing method in this research. While only a 1.02% increase in accuracy was gained using pre-processing methods in the first stage classification, an increase of 26.75% was gained in the second stage classification. This shows that pre-processing causes the classifiers to improve their analysis more so on complex classifications than simple classifications.

Complex canopy classification

Discerning a complex canopy was not difficult because of the hyperspectral data provided and the pre-processing and classifiers used. While the concern that species similarities would confuse the classification, it was not evident as three oak species were correctly discerned in the classification. The SVM classifier outperformed the other classifiers in this discernment of a complex canopy allowing for use by urban forest managers in analysing of the tree species locations.

Accuracy Interpretation

The Stage Two results had limited practical use because although the classifiers could accurately discern between the twenty-tree species, they also included all other species into the twenty classes. Therefore, to make an image that is more useful in visual assessments and quantitative analysis, additional classes for individual or multiple species should be made in future work to maximise the use of such a classification for a tree inventory. This classification showed that the twenty species were distinct enough to be separated properly.

Future research

This research leaves many unanswered questions that could be the focus of future work.

- How many additional classes of tree species can be used in one classification and still maintain an overall accuracy of >90%?

- What other tree characteristics, that are collected for tree inventories, can be identified through remote sensing?
- What changes in pre-processing can be made to improve classifications?
- Are there significant similarities between certain species that prevent accuracy classification?
- What is the minimum amount of training data needed and does it vary between classes?

Final remarks

This research's outcome supports and agrees with the initial hypothesis that pre-processing and analysis of information gathered by the aisaFENIX sensor can separate twenty tree species to an overall accuracy of >90% within an urban environment using a small training data set. This highlights how hyperspectral remote sensing is a practical alternative method for creating tree inventories. In a highly diverse urban forest, additional work is needed for quantitative and visual assessments to give exact locations and identification of tree species. This will help managers form visions, set goals and help them in their management decisions which will in turn support the preservation and health of the ecosystem.

7.0 References

Akpinar, A., Barbosa-Leiker, Celestina, & Brooks, K. R. (2016). Does green space matter? Exploring relationships between green space type and health indicators. Urban Forestry & Urban Greening, 20, 407-418. doi:http://dx.doi.org/10.1016/j.ufug.2016.10.013

Alonzo, M., Bookhagen, B., & Roberts, D. A. (2014). Urban tree species mapping using hyperspectral and lidar data fusion. Remote Sensing of Environment, 148, 70-83. doi:http://dx.doi.org/10.1016/j.rse.2014.03.018

Alonzo, M., McFadden, J. P., Nowak, D. J., & Roberts, D. A. (2016). Mapping urban forest structure and function using hyperspectral imagery and lidar data. Urban Forestry & Urban Greening, 17, 135-147. doi:http://dx.doi.org/10.1016/j.ufug.2016.04.003

Alvey, A. A. (2006). Promoting and preserving biodiversity in the urban forest. Urban Forestry & Urban Greening, 5(4), 195-201. doi:http://dx.doi.org/10.1016/j.ufug.2006.09.003

Archibald, R., & Fann, G. (2007). Feature Selection and Classification of Hyperspectral Images With Support Vector Machines. IEEE Geoscience and Remote Sensing Letters, 4(4), 674-677. doi:10.1109/LGRS.2007.905116

Armson, D., Stringer, P., & Ennos, A. R. (2013). The effect of street trees and amenity grass on urban surface water runoff in Manchester, UK. Urban Forestry and Urban Greening, 12(3), 282-286. doi:10.1016/j.ufug.2013.04.001

Arnberger, A., & Eder, R. (2015). Are urban visitors' general preferences for green spaces similar to their preferences when seeking stress relief? Urban Forestry & Urban Greening, 14(4), 872-882. doi:http://dx.doi.org/10.1016/j.ufug.2015.07.005

Arnberger, A., Schneider, I. E., Ebenberger, M., Eder, R., Venette, R. C., Snyder, S. A., . . . Cottrell, S. (2017). Emerald ash borer impacts on visual preferences for urban forest recreation

settings. Urban Forestry & Urban Greening, 27(Supplement C), 235-245. doi:https://doi.org/10.1016/j.ufug.2017.08.004

Arnfield, A. J. (2003). Two decades of urban climate research: A review of turbulence, exchanges of energy and water, and the urban heat island. International Journal of Climatology, 23(1), 1-26. doi:10.1002/joc.859

Baldauf, R. (2017). Roadside vegetation design characteristics that can improve local, near-road air quality. Transportation Research Part D: Transport and Environment, 52, 354-361. doi:10.1016/j.trd.2017.03.013

Boardman, J. W. K., F. A. (1994). Automated spectral analysis: a geological example using AVIRIS data, north Grapevine Mountains, Nevada. Proceedings, ERIM Tenth Thematic Conference on Geologic Remote Sensing, 407-418.

Bolund, P., & Hunhammar, S. (1999). Ecosystem services in urban areas. Ecological Economics, 29(2), 293-301. doi:10.1016/S0921-8009(99)00013-0

Chen, Y.-C., & Su, C.-T. (2016). Distance-based margin support vector machine for classification. Applied Mathematics and Computation, 283, 141-152. doi:http://dx.doi.org/10.1016/j.amc.2016.02.024

Chen, Y., Wang, X., Jiang, B., Yang, N., & Li, L. (2016). Pavement induced soil warming accelerates leaf budburst of ash trees. Urban Forestry & Urban Greening, 16, 36-42. doi:http://dx.doi.org/10.1016/j.ufug.2016.01.014

Cho, M. A., Mathieu, R., Asner, G. P., Naidoo, L., van Aardt, J., Ramoelo, A., . . . Erasmus, B. (2012). Mapping tree species composition in South African savannas using an integrated airborne spectral and LiDAR system. Remote Sensing of Environment, 125, 214-226. doi:http://dx.doi.org/10.1016/j.rse.2012.07.010

Clark, J., & Matheny, M. (1991). Management of Mature Trees. Journal of Arboriculture, 17(7), 173-184.

Coombes, E., Jones, A. P., & Hillsdon, M. (2010). The relationship of physical activity and overweight to objectively measured green space accessibility and use. Social Science and Medicine, 70(6), 816-822. doi:10.1016/j.socscimed.2009.11.020

Dalponte, M., Bruzzone, L., & Gianelle, D. (2008). Fusion of Hyperspectral and LIDAR Remote Sensing Data for Classification of Complex Forest Areas. IEEE Transactions on Geoscience and Remote Sensing, 46(5), 1416-1427. doi:10.1109/TGRS.2008.916480

Dalponte, M., Bruzzone, L., & Gianelle, D. (2012). Tree species classification in the Southern Alps based on the fusion of very high geometrical resolution multispectral/hyperspectral images and LiDAR data. Remote Sensing of Environment, 123, 258-270. doi:http://dx.doi.org/10.1016/j.rse.2012.03.013

de Boves Harrington, P. (2017). Support vector machine classification trees based on fuzzy entropy of classification. Analytica Chimica Acta, 954, 14-21. doi:https://doi.org/10.1016/j.aca.2016.11.072

Demetriades-Shah, T. H., Steven, M. D., & Clark, J. A. (1990). High resolution derivative spectra in remote sensing. Remote Sensing of Environment, 33(1), 55-64. doi:http://dx.doi.org/10.1016/0034-4257(90)90055-Q

Donovan, G. H., & Butry, D. T. (2009). The value of shade: Estimating the effect of urban trees on summertime electricity use. Energy and Buildings, 41(6), 662-668. doi:10.1016/j.enbuild.2009.01.002

Du, P., Tan, K., & Xing, X. (2012). A novel binary tree support vector machine for hyperspectral remote sensing image classification. Optics Communications, 285(13–14), 3054-3060. doi:http://dx.doi.org/10.1016/j.optcom.2012.02.092

Fassnacht, F. E., Latifi, H., Stereńczak, K., Modzelewska, A., Lefsky, M., Waser, L. T., . . . Ghosh, A. (2016). Review of studies on tree species classification from remotely sensed data. Remote Sensing of Environment, 186, 64-87. doi:http://dx.doi.org/10.1016/j.rse.2016.08.013

Ferreira, M. P., Zortea, M., Zanotta, D. C., Shimabukuro, Y. E., & de Souza Filho, C. R. (2016). Mapping tree species in tropical seasonal semi-deciduous forests with hyperspectral and multispectral data. Remote Sensing of Environment, 179, 66-78. doi:http://dx.doi.org/10.1016/j.rse.2016.03.021

Foody, G. (2004). Thematic Map Comparison: Evaluating the Statistical Significance of Differences in Classification Accuracy (Vol. 70).

Franco, J. A., Bañón, S., Vicente, M. J., Miralles, J., & Martínez-Sánchez, J. J. (2011). Root development in horticultural plants grown under abiotic stress conditions - a review. Journal of Horticultural Science and Biotechnology, 86(6), 543-556. Retrieved from https://www.scopus.com/inward/record.uri?eid=2-s2.0-80955150865&partnerID=40&md5=273fa166467545f144cffb9b65b34197

Fraser, C. S., Woods, A., & Brizzi, D. (2005). Hyper redundancy for accuracy enhancement in automated close range photogrammetry. Photogrammetric Record, 20(111), 205-217. doi:10.1111/j.1477-9730.2005.00327.x

Ghiyamat, A., & Shafri, H. Z. M. (2010). A review on hyperspectral remote sensing for homogeneous and heterogeneous forest biodiversity assessment. International Journal of Remote Sensing, 31(7), 1837-1856. doi:10.1080/01431160902926681

Ghosh, A., Fassnacht, F. E., Joshi, P. K., & Koch, B. (2014). A framework for mapping tree species combining hyperspectral and LiDAR data: Role of selected classifiers and sensor across three spatial scales. International Journal of Applied Earth Observation and Geoinformation, 26, 49-63. doi:http://dx.doi.org/10.1016/j.jag.2013.05.017

Gibbons, K. H., & Ryan, C. M. (2015). Characterizing comprehensiveness of urban forest management plans in Washington State. Urban Forestry & Urban Greening, 14(3), 615-624. doi:http://dx.doi.org/10.1016/j.ufug.2015.06.003

Green, A. A. B., M.; Switzer, P.; Craig, M. D. (1988). A transformation for ordering multispectral data in terms of image quality with implications for noise removal. IEEE Transactions on Geoscience and Remote Sensing, 26(1), 65-74.

Harris. (2017). Classification Tools. Retrieved from http://www.harrisgeospatial.com/docs/ClassificationTools.html

Jia, X., & Richards, J. A. (1993). Binary coding of imaging spectrometer data for fast spectral matching and classification. Remote Sensing of Environment, 43(1), 47-53. doi:http://dx.doi.org/10.1016/0034-4257(93)90063-4

Jim, C. Y., & Chen, W. Y. (2008). Assessing the ecosystem service of air pollutant removal by urban trees in Guangzhou (China). Journal of Environmental Management, 88(4), 665-676. doi:10.1016/j.jenvman.2007.03.035

Jones, T. G., Coops, N. C., & Sharma, T. (2010). Assessing the utility of airborne hyperspectral and LiDAR data for species distribution mapping in the coastal Pacific Northwest, Canada. Remote Sensing of Environment, 114(12), 2841-2852. doi:http://dx.doi.org/10.1016/j.rse.2010.07.002

Kefauver, S., Penuelas, J., & Ustin, S. (2012). Applications of hyperspectral remote sensing and GIS for assessing forest health and air pollution.

Koch, B. (2010). Status and future of laser scanning, synthetic aperture radar and hyperspectral remote sensing data for forest biomass assessment. ISPRS Journal of Photogrammetry and Remote Sensing, 65(6), 581-590. doi:https://doi.org/10.1016/j.isprsjprs.2010.09.001

Koeser, A. K., Gilman, E. F., Paz, M., & Harchick, C. (2014). Factors influencing urban tree planting program growth and survival in Florida, United States. Urban Forestry and Urban Greening, 13(4), 655-661. doi:10.1016/j.ufug.2014.06.005

Kuo, F. E., & Sullivan, W. C. (2001). Environment and crime in the inner city does vegetation reduce crime? Environment and Behavior, 33(3), 343-367. doi:10.1177/00139160121973025

Laćan, I., & McBride, J. R. (2008). Pest Vulnerability Matrix (PVM): A graphic model for assessing the interaction between tree species diversity and urban forest susceptibility to insects and diseases. Urban Forestry and Urban Greening, 7(4), 291-300. doi:10.1016/j.ufug.2008.06.002

Liu, L., Coops, N. C., Aven, N. W., & Pang, Y. (2017). Mapping urban tree species using integrated airborne hyperspectral and LiDAR remote sensing data. Remote Sensing of Environment, 200(Supplement C), 170-182. doi:https://doi.org/10.1016/j.rse.2017.08.010

Lucas, R., Bunting, P., Paterson, M., & Chisholm, L. (2008). Classification of Australian forest communities using aerial photography, CASI and HyMap data. Remote Sensing of Environment, 112(5), 2088-2103. doi:http://dx.doi.org/10.1016/j.rse.2007.10.011

Mace, G. M., Norris, K., & Fitter, A. H. (2012). Biodiversity and ecosystem services: a multilayered relationship. Trends in Ecology & Evolution, 27(1), 19-26. doi:http://dx.doi.org/10.1016/j.tree.2011.08.006

Martínez, S., Ortiz, J., Gil, M. L., & Rego, M. T. (2013). Recording complex structures using close range photogrammetry: The cathedral of santiago de compostela. Photogrammetric Record, 28(144), 375-395. doi:10.1111/phor.12040

McPherson, E. G. (2007). Benefit-based tree valuation. Arboriculture and Urban Forestry, 33(1), 1-11. Retrieved from https://www.scopus.com/inward/record.uri?eid=2-s2.0-33846392933&partnerID=40&md5=4a5b2fffa30f803774fb8efa7cd50cc3

Miller, R. W. (1997). Urban Forestry: Planning and Managing Urban Greenspaces: Prentice Hall.

Mitchell, R. (2013). Is physical activity in natural environments better for mental health than physical activity in other environments? Social Science and Medicine, 91, 130-134. doi:10.1016/j.socscimed.2012.04.012

Morgenroth, J., Östberg, J., Konijnendijk van den Bosch, C., Nielsen, A. B., Hauer, R., Sjöman, H., . . . Jansson, M. (2016). Urban tree diversity—Taking stock and looking ahead. Urban Forestry & Urban Greening, 15, 1-5. doi:http://dx.doi.org/10.1016/j.ufug.2015.11.003

Mullaney, J., Lucke, T., & Trueman, S. J. (2015). A review of benefits and challenges in growing street trees in paved urban environments. Landscape and Urban Planning, 134, 157-166. doi:http://dx.doi.org/10.1016/j.landurbplan.2014.10.013

Nowak, D. J., Kuroda, M., & Crane, D. E. (2004). Tree mortality rates and tree population projections in Baltimore, Maryland, USA. Urban Forestry & Urban Greening, 2(3), 139-147. doi:http://dx.doi.org/10.1078/1618-8667-00030

Nowak, D. J., Walton, J. T., Stevens, J. C., Crane, D. E., & Hoehn, R. E. (2008). Effect of plot and sample size on timing and precision of urban forest assessments. Arboriculture and Urban Forestry, 34(6), 386-390. Retrieved from

https://www.scopus.com/inward/record.uri?eid=2-s2.0-56449089909&partnerID=40&md5=adb4c098c97ffce8b23355908c51e5fe

Ogen, Y., Goldshleger, N., & Ben-Dor, E. (2017). 3D spectral analysis in the VNIR–SWIR spectral region as a tool for soil classification. Geoderma, 302, 100-110. doi:http://dx.doi.org/10.1016/j.geoderma.2017.04.020

Ordóñez-Barona, C. (2015). Adopting public values and climate change adaptation strategies in urban forest management: A review and analysis of the relevant literature. Journal of Environmental Management, 164, 215-221. doi:http://dx.doi.org/10.1016/j.jenvman.2015.09.004

Pandit, R., & Laband, D. N. (2010). Energy savings from tree shade. Ecological Economics, 69(6), 1324-1329. doi:10.1016/j.ecolecon.2010.01.009

Pham, L. T. H., Brabyn, L., & Ashraf, S. (2016). Combining QuickBird, LiDAR, and GIS topography indices to identify a single native tree species in a complex landscape using an object-based classification approach. International Journal of Applied Earth Observation and Geoinformation, 50, 187-197. doi:http://dx.doi.org/10.1016/j.jag.2016.03.015

Pullanagari, R. R., Kereszturi, G., & Yule, I. J. (2016). Mapping of macro and micro nutrients of mixed pastures using airborne AisaFENIX hyperspectral imagery. ISPRS Journal of Photogrammetry and Remote Sensing, 117, 1-10. doi:http://dx.doi.org/10.1016/j.isprsjprs.2016.03.010

Rhodes, J. R., Ng, C. F., de Villiers, D. L., Preece, H. J., McAlpine, C. A., & Possingham, H. P. (2011). Using integrated population modelling to quantify the implications of multiple threatening processes for a rapidly declining population. Biological Conservation, 144(3), 1081-1088. doi:10.1016/j.biocon.2010.12.027

Richards, J. A. (1999). Remote Sensing Digital Image Analysis: Springer-Verlag.

Richter, R., Reu, B., Wirth, C., Doktor, D., & Vohland, M. (2016). The use of airborne hyperspectral data for tree species classification in a species-rich Central European forest area. International Journal of Applied Earth Observation and Geoinformation, 52, 464-474. doi:http://dx.doi.org/10.1016/j.jag.2016.07.018

Salmond, J. A., Tadaki, M., Vardoulakis, S., Arbuthnott, K., Coutts, A., Demuzere, M., . . . Wheeler, B. W. (2016). Health and climate related ecosystem services provided by street trees in the urban environment. Environmental Health, 15(1), S36. doi:10.1186/s12940-016-0103-6

Samson, R. (2017). The Urban Forest: Cultivating Green Infrastructure for People and the Environment. In C. C. David Pearlmutter, Roeland Samson, Liz O'Brien, Silvija Krajter Ostoić, Giovanni Sanesi, Rocío Alonso del Amo (Ed.): Springer International Publishing.

Schlerf, M., Atzberger, C., Hill, J., Buddenbaum, H., Werner, W., & Schüler, G. (2010). Retrieval of chlorophyll and nitrogen in Norway spruce (Picea abies L. Karst.) using imaging spectroscopy. International Journal of Applied Earth Observation and Geoinformation, 12(1), 17-26. doi:10.1016/j.jag.2009.08.006

Schmitt-Harsh, M., Mincey, S. K., Patterson, M., Fischer, B. C., & Evans, T. P. (2013). Private residential urban forest structure and carbon storage in a moderate-sized urban area in the Midwest, United States. Urban Forestry & Urban Greening, 12(4), 454-463. doi:http://dx.doi.org/10.1016/j.ufug.2013.07.007

Shang, X., & Chisholm, L. A. (2014). Classification of Australian native forest species using hyperspectral remote sensing and machine-learning classification algorithms. IEEE Journal of Selected Topics in Applied Earth Observations and Remote Sensing, 7(6), 2481-2489. doi:10.1109/JSTARS.2013.2282166

Smith, M.-L., Ollinger, S. V., Martin, M. E., Aber, J. D., Hallett, R. A., & Goodale, C. L. (2002). DIRECT ESTIMATION OF ABOVEGROUND FOREST PRODUCTIVITY THROUGH HYPERSPECTRAL REMOTE SENSING OF CANOPY NITROGEN. Ecological Applications, 12(5), 1286-1302. doi:10.1890/1051-0761(2002)012[1286:DEOAFP]2.0.CO;2

Thomlinson, J. R., Bolstad, P. V., & Cohen, W. B. (1999). Coordinating Methodologies for Scaling Landcover Classifications from Site-Specific to Global. Remote Sensing of Environment, 70(1), 16-28. doi:http://dx.doi.org/10.1016/S0034-4257(99)00055-3

Toth, C., & Jóźków, G. (2016). Remote sensing platforms and sensors: A survey. ISPRS Journal of Photogrammetry and Remote Sensing, 115, 22-36. doi:http://dx.doi.org/10.1016/j.isprsjprs.2015.10.004

Treitz, P. M., & Howarth, P. J. (1999). Hyperspectral remote sensing for estimating biophysical parameters of forest ecosystems. Progress in Physical Geography, 23(3), 359-390. doi:10.1177/030913339902300303

United-Nations. (2014). World urbanisation prospects. Retrieved from https://esa.un.org/unpd/wup/publications/files/wup2014-highlights.Pdf

van Dillen, S. M. E., de Vries, S., Groenewegen, P. P., & Spreeuwenberg, P. (2012). Greenspace in urban neighbourhoods and residents' health: adding quality to quantity. Journal of Epidemiology and Community Health, 66(6), e8. doi:10.1136/jech.2009.104695

Vogt, J., Gillner, S., Hofmann, M., Tharang, A., Dettmann, S., Gerstenberg, T., . . . Roloff, A. (2017). Citree: A database supporting tree selection for urban areas in temperate climate. Landscape and Urban Planning, 157, 14-25. doi:http://dx.doi.org/10.1016/j.landurbplan.2016.06.005

Vogt, J. M., Watkins, S. L., Mincey, S. K., Patterson, M. S., & Fischer, B. C. (2015). Explaining planted-tree survival and growth in urban neighborhoods: A social-ecological approach to studying recently-planted trees in Indianapolis. Landscape and Urban Planning, 136, 130-143. doi:10.1016/j.landurbplan.2014.11.021

Wolch, J., Jerrett, M., Reynolds, K., McConnell, R., Chang, R., Dahmann, N., . . . Berhane, K. (2011). Childhood obesity and proximity to urban parks and recreational resources: A longitudinal cohort study. Health and Place, 17(1), 207-214. doi:10.1016/j.healthplace.2010.10.001

Xiang, S., Nie, F., & Zhang, C. (2008). Learning a Mahalanobis distance metric for data clustering and classification. Pattern Recognition, 41(12), 3600-3612. doi:http://dx.doi.org/10.1016/j.patcog.2008.05.018

Xie, H., & Tong, X. (2012, 4-7 June 2012). An inproved binary encoding algorithm for classification of hyperspectral images. Paper presented at the 2012 4th Workshop on Hyperspectral Image and Signal Processing: Evolution in Remote Sensing (WHISPERS).

Youngentob, K. N., Roberts, D. A., Held, A. A., Dennison, P. E., Jia, X., & Lindenmayer, D. B. (2011). Mapping two Eucalyptus subgenera using multiple endmember spectral mixture analysis and continuum-removed imaging spectrometry data. Remote Sensing of Environment, 115(5), 1115-1128. doi:http://dx.doi.org/10.1016/j.rse.2010.12.012

Zhang, C., & Qiu, F. (2012). Mapping individual tree species in an urban forest using airborne lidar data and hyperspectral imagery: AAG remote sensing specialty group 2011 award winner. Photogrammetric Engineering and Remote Sensing, 78(10), 1079-1087. Retrieved from https://www.scopus.com/inward/record.uri?eid=2-s2.0-84868023232&partnerID=40&md5=3ed391db71b6210c0c0db5c3bd9b080a

Zhang, Y., & Mishra, R. K. (2012). A review and comparison of commercially available pan-sharpening techniques for high resolution satellite image fusion. Paper presented at the 2012 IEEE International Geoscience and Remote Sensing Symposium.